Biochimica et Biophysica Acta, 443 (1976) 143–155

BBA 77390

FREEZE-FRACTURE ELECTRON MICROSCOPY OF PREEXISTING AND NASCENT CELL MEMBRANE IN CLEAVING EGGS OF *XENOPUS LAEVIS*

JOHN G. BLUEMINK[a,*], LEON G. J. TERTOOLEN[a], PIET H. J. Th. VERVERGAERT[b] and ARIE J. VERKLEIJ[b]

[a]*Hubrecht Laboratory, International Embryological Institute, Utrecht and* [b]*the Biological Ultrastructure Research Unit of the State University, Utrecht (The Netherlands)*

(Received January 13th, 1976)

SUMMARY

During cell division in the *Xenopus* egg (diameter 1.25 mm) new cell membrane is formed in the furrow region (rate of growth approx $4 \cdot 10^4$ μm^2/min). Freeze-fracture electron microscopy has produced the following data. Preexisting plasma membrane faces show a reversed polarity with respect to particle distribution, i.e. more particles are attached to the E-face (density 1600–2200 particles/μm^2) than to the P-face (300 particles/μm^2). A frequency histogram of 2331 measured intramembranous particles does not show a continuous range of sizes. The following sizes were very obvious: 95 Å (12 %), 125 Å (30 %) and 180 Å (6 %). At the tips of surface protrusions both the E- and the P-face are particle-free. Nascent cell membrane fracture faces are more difficult to obtain. The particle density is low (E-face 300–500 particles/μm^2). Lowering the ambient temperature to 5 °C for approx. 5 mins does not change the normal particle pattern, but it improves the output in nascent membrane fracture faces. The fact that in the *Xenopus* egg preexisting and nascent membrane regions are continuous but nevertheless maintain their highly different particle densities is noteworthy. The freeze-fracture data are discussed in relation to, among other things, the known values of the specific resistances of these membrane regions.

INTRODUCTION

Xenopus eggs are large cells (diameter 1.25 mm) which undergo complete cleavage. They have been used to analyse the process of new (nascent) membrane formation during cytokinesis [1–3]. Evidence exists that nascent membrane is formed during and not before or after cleavage, and that it grows in the furrow region only.

The preexisting and the nascent cell membrane in *Xenopus* eggs differ in various respects. The surface occupied by the preexisting membrane is rough and pigmented and is underlain by a cortical cytoplasmic layer of filamentous material

* Address for request of reprints: Dr. J. G. Bluemink, Hubrecht Laboratory, Uppsalalaan 8, Utrecht, The Netherlands.

[1–6]. In ultrathin sections the membrane itself exhibits a well-defined tri-lamellar organization [1]. The specific resistance of this membrane is known to be 74 $k\Omega \cdot cm^2$, a high value in comparison with many other biological membranes [2].

The surface of the nascent cell membrane area is smooth and virtually without underlying pigment [1–4]. In ultrathin sections this membrane exhibits an ill-defined tri-lamellar organization and no filamentous material is associated with it [1]. The specific resistance is known to be 1.82 $k\Omega \cdot cm^2$, which means that the membrane is highly permeable for ions [2].

When cleaving eggs are exposed to cytochalasin B the furrow is caused to regress [1, 2, 4, 6]. As a result the interblastomeric surface, i.e. the nascent membrane is exposed (Fig. 1b). Seemingly unimpeded growth of nascent membrane has been observed [1] in cytochalasin-treated eggs devoid of their vitelline envelope (Fig. 1c). Normally cleaving eggs inside their vitelline envelope assemble $1.4 \cdot 10^6$ μm^2 of interblastomeric membrane to complete the first cell division [1, 2], which means that nascent membrane forms at a rate of $4 \cdot 10^4$ μm^2/min.

Viewed under the dissecting microscope the area of nascent cell membrane is clearly distinct from the preexisting cell membrane. Although initially the boundary between the two areas is diffuse, approx. 12 min after the onset of cleavage it becomes marked by a distinct pigmented ridge protruding from the egg surface [1, 2, 4]. As a result preexisting and nascent cell membrane areas can be recognized with certainty after freeze-fracturing. Therefore cytochalasin-treated *Xenopus* eggs may be expected to offer favourable material for freeze-fracture analysis of de novo cell membrane formation.

MATERIALS AND METHODS

Material. Eggs of *Xenopus laevis* were collected in the laboratory from hormonally stimulated couples as described earlier [6]. The jelly capsule was chemically removed using 2% L-cysteine/HCl plus 0.2% papain in Steinberg solution [7], pH 7.8 (modified according to Spiegel, ref. 8). As a control for the decapsulation by prote-oly-

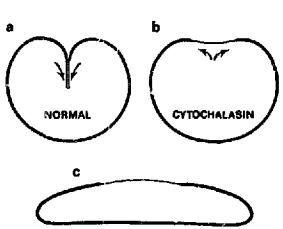

Fig. 1. *Xenopus* egg in cross section. (a) Normal egg with ingrowing furrow. (b) Cytochalasin-treated egg with regressed furrow; the interblastomeric surface has become part of the external surface. (c) Cytochalasin-treated egg flattened by gravity after removal of the vitelline envelope. As in (b) the interblastomeric surface is external.

tic enzyme digestion, eggs were also decapsulated mechanically with forceps, in this case after prior fixation in aldehyde.

After removal of the vitelline envelope with forceps, living eggs flatten under gravity (Fig. 1). These eggs were kept in Steinberg solution in Falcon petri dishes with a 2 % agar bottom.

Fixation. Eggs devoid of their vitelline envelope were exposed to 10 μg/ml cytochalasin B in Steinberg solution at the onset of cleavage (SS-stage, see ref. 4). As soon as the nascent cell membrane area (unpigmented surface) became well-delimited from the preexisting cell membrane (pigmented surface) about 12 min later (Fig. 2a), the flattened eggs were fixed in 2.50 % glutaraldehyde, 1 % acrolein in 0.05 M cacodylate buffer pH 7.2 (room temperature). The fixation time was 1.5 h. As a control for the cytochalasin treatment a number of untreated eggs were also prepared for freeze-fracturing.

Chilling experiment. To analyse the effect of chilling on the particle pattern of the membrane, eggs exposed to cytochalasin B for 10 min at room temperature

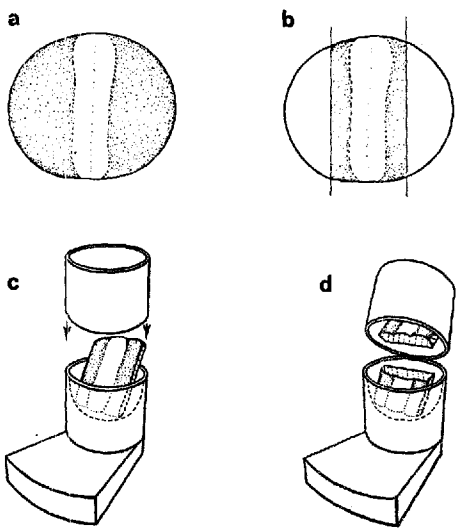

Fig. 2. (a) Top view of a cytochalasin-treated egg flattened by gravity. Mid region: regressed furrow with nascent cell membrane. Lateral parts: preexisting cell membrane. (b) As in (a) the lines indicate removal of lateral portions. (c) Remaining part positioned in a specimen holder. (d) Situation after freeze-fracturing.

were quickly chilled to approx. 5 °C and kept at that temperature for approx. 5 min. They were then aldehyde-fixed in the cold and kept at the same low temperature till the moment of freezing.

Freeze-fracturing. On both sides of the nascent membrane area of the flattened egg lateral portions covered by preexisting cell membrane were cut away (Fig. 2b). The remaining part was equilibrated against 20 % glycerol in 0.05 M cacodylate buffer for at least 2 h. For freeze-fracturing the egg part was then positioned in a specimen holder (Denton Vacuum Inc., Cherry Hill, N.Y.) in such a way that the fracture plane would always split adjacent regions of preexisting and nascent membrane in a direction across their border line (Fig. 2c, d). The cylindrical upper part of the specimen holder was placed in position and excess fluid was removed with filter paper. The specimen holder was transferred in an upright position with a pair of forceps, rapidly immersed into a thawed layer of nitrogen and pressed against the solid, colder nitrogen underneath [9]. Fracturing, etching and coating were carried out at −100 °C in a vacuum of better than 10^{-6} Torr in a Denton instrument (type D.F.E.-3) equipped with a Balzers electron bombardment unit.

Electron microscopy. The platinum/carbon-coated replicas were cleaned by exposing them to a 1 : 1 mixture of 10 % potassium bichromate/98 % sulphuric acid at room temperature for 1 h, then to 1 M sodium hydroxide for 72 h at a temperature of 55 °C. Finally they were rinsed in distilled water and collected on single-hole (1 × 2 mm) grids (Fig. 3) covered with a carbon-coated supporting film of Pioloform F [10]. The replicas were inspected in a Zeiss EM 10 electron microscope at acceleration voltages of 80 or 100 kV.

The abbreviations E-face and P-face are used, respectively to indicate the exposed core region of the membrane on the extracellular side, and its mirror image on the protoplasmic side, as proposed by Branton et al. [11]. The interpretation regarding the position of the fracture plane is based on Branton's fracturing model which holds that the membrane is split along the apolar interior. The arguments for making this assumption are 2-fold. (1) Consistently, only two types of fracture faces were found in the uncleaved *Xenopus* egg. The structure of the two fracture faces indicate that they are complementary. One face has predominantly particles (diameter approx. 75–185 Å) attached to it, the other face is dominated by relatively large pits (diameter approx.

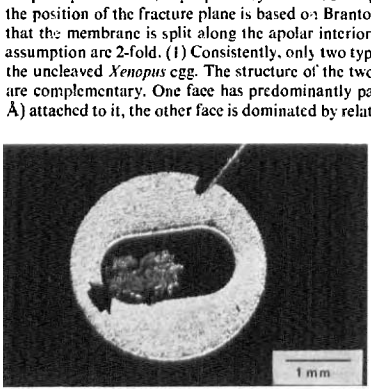

Fig. 3. Replica (arrow) carried by a supporting film on a single-hole grid.

Fig. 4. External fracture face (E-face) of preexisting membrane (EF). Direction of shadowing indicated by encircled arrowhead. The particle-free regions are surface protrusions (SP). Magnification × 56 250. Inset: four intramembranous particles of the 75, 95, 125 and 180 Å class are indicated. Magnification 216 000.

80–135 Å). (2) Besides these two types, no other type of fracture face has been observed.

Particle sizes were determined by measuring the widest part of the shadow at right angles to the direction of the shadow. Methods of measuring and sampling were as described by Goodenough and Stachelin [12].

RESULTS

Fig. 4 shows a plasma membrane fracture face with many particles attached to it. Micrographs (magnification ×160 000) of replicas like this one were used to determine the relative frequencies of particle sizes. Fig. 5 presents the frequency histogram for 2331 intramembranous particles in the preexisting plasma membrane. On the assumption that the values obtained could represent a continuous range of particle sizes, the smooth normal curve was computed from the sample mean ($\mu = 1.90$ mm) and the variance ($d = 0.33$). When tested for non-normality, the discrepancy between the observed and expected frequencies turned out to be highly significant ($DF = 17$, $X^2 = 1307.57$, $P < 0.001$). Thus, the histogram represents more than one class of intramembranous particles. Three size classes covering a reasonable percentage of the total number stood out. They contained particles of 95, 125 and 180 Å, and represent 12 %, 30 %, and 6 % of the total population, respectively. Particles of "conventional" size (approx. 75 Å) were present, but represented only 2 % of the total number. The inset in Fig. 4 shows particles of the four classes mentioned at high magnification.

The fracture faces of the preexisting membrane showed a reversed polarity as compared with the distribution of particles found in the plasma membrane of most eukaryotic cells, that is to say more particles were associated with the E-face than with the P-face. This could be established on the basis of membrane fracture faces of sur-

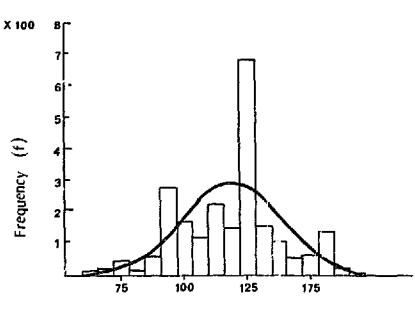

Fig. 5. Size-frequency histogram of intramembranous particles in preexisting membrane. The data have been converted from measurements on micrographs (magnification × 160 000) which were orginally grouped at intervals of 0.1 mm. The corresponding diameters of the particles are indicated.

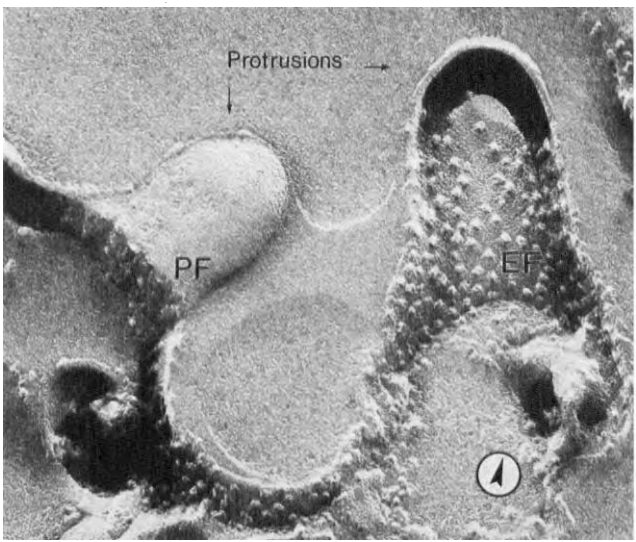

Fig. 6. Freeze fracture faces of surface protrusions. The concave fracture shows the E-face (EF), the convex fracture the P-face (PF) of the preexisting membrane. Magnification × 160 000.

face protrusions. Fig. 6 presents an example. The direction of shadowing is indicated and implies that one fracture face is concave and thus exposes the inner side of the external leaflet (E-face), whereas the other fracture face is convex and exposes the inner side of the protoplasmic leaflet (P-face) of the plasma membrane. As a rule the E-face of surface protrusions showed a particle density equal to that of the rest of the preexisting membrane (1600–2200 particles/μm^2) except for the most distal end. Here the E-face was frequently found to be particle-free (see also Fig. 4). The P-face of preexisting membrane was characterised by a great many depressions or pits (Fig. 7) and a small number of particles (density approx. 300 particles/μm^2). These particles were less conspicuous than those of the E-face, the majority falling in the size class of $\leq$ 95 Å (inset Fig. 7).

The eggs were routinely decapsulated by proteolytic enzyme treatment. The possibility was considered that this treatment could have given rise to the unusually large particles. As a control, eggs were fixed and decapsulated manually with forceps, and prepared for freeze-fracturing. The particles associated with the E-face of the preexisting membrane were examined (Fig. 8) and it was found that their sizes were very similar to those of the particles seen in chemically decapsulated eggs.

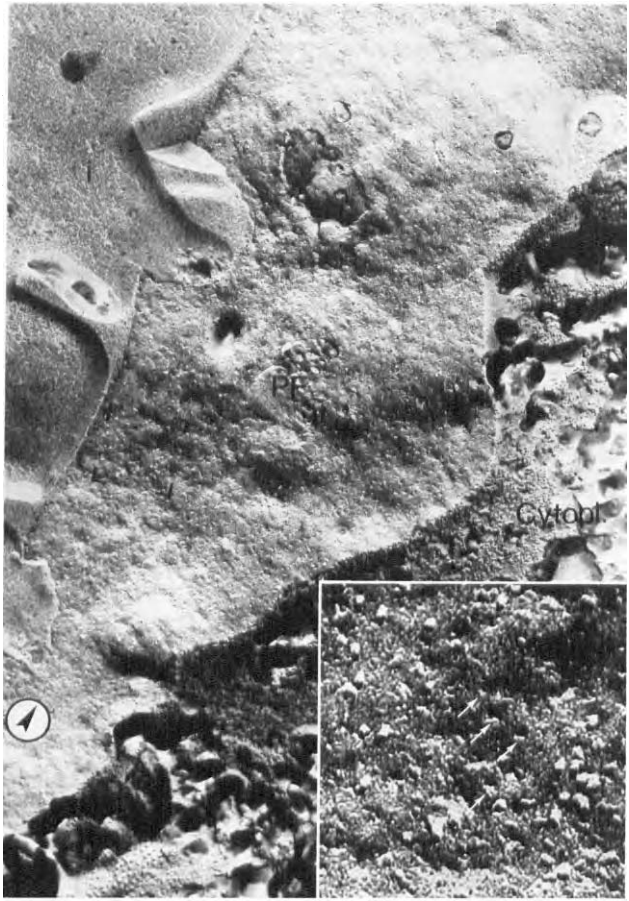

Fig. 7. Fracture face of a vesiculating membrane showing the inner side of the protoplasmic leaflet (PF). Magnification ca. 250. Inset: particles of ca. 95 Å, and pits (arrows). Magnification 236 000.

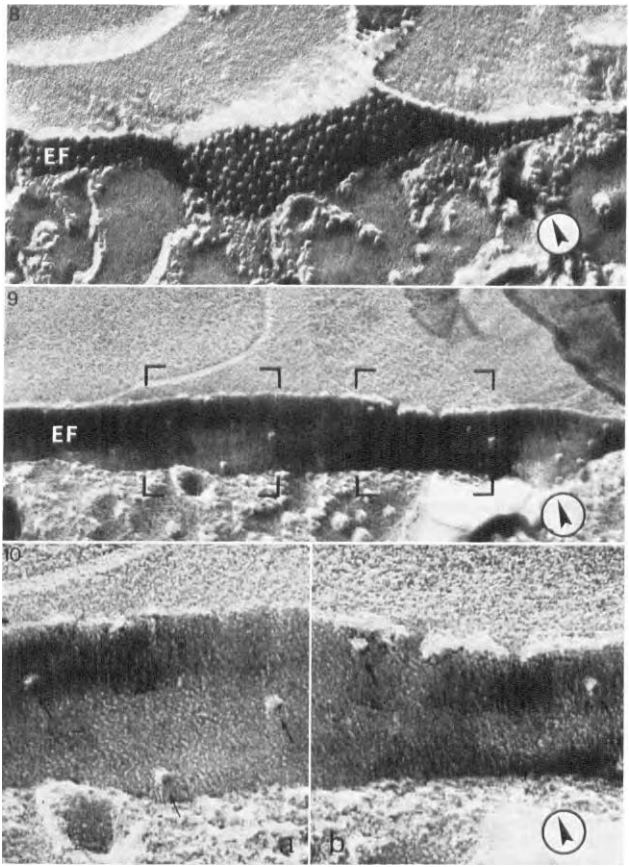

Fig. 8. E-face of preexisting membrane (EF) of a manually decapsulated egg not exposed to cytochalasin B. Magnification × 100 000.

Fig. 9. E-face of nascent membrane (EF) of an egg chilled for 5 min at approx. 5 °C. The low particle density is representative for the nascent membrane fracture faces seen. Magnification × 100 000.

Fig. 10. E-face of nascent membrane. Marked areas shown in Fig. 9 at higher magnification (× 240 000). Particles of various sizes are indicated.

In contrast to the preexisting membrane, the yield of fracture faces of nascent membrane was low, i.e. only small areas were exposed. Fig. 9 shows the E-face of the nascent cell membrane, which has a particle density of approx. 300–500 particles/μm^2. The particles were always randomly distributed and not uniform in size (Fig. 10a, b). All the various particle sizes observed in the preexisting membrane could also be found in nascent membrane faces. The observed difference in particle density between the preexisting and the nascent cell membrane was unambiguous and very characteristic.

As a control for the cytochalasin treatment, eggs not exposed to the drug were prepared for freeze-fracturing. The density and distribution of the particles associated with the E-face of the preexisting membrane were examined. There was no difference with treated eggs. Also in these eggs the E-face in the apical parts of surface protrusions was particle-free.

Lowering of the ambient temperature can induce a rearrangement of intramembranous particles in an intact organism (see Discussion). In order to get an impression of the degree of mobility of intramembranous particles, eggs were exposed to an ambient temperature of approx. 5 °C for about 5 min. Fracture faces (E-face) of preexisting and nascent membrane were inspected, but clustering or aggregation of particles were not observed. However, chilling did have another striking effect: the nascent membrane split over much larger areas than in unchilled eggs.

DISCUSSION

Freeze-fracture electron microscopy of cleaving *Xenopus* eggs has produced the following data. Intramembranous particles range in size from approx. 70–180 Å. Preexisting membrane fracture faces show a reversed polarity in particle distribution, i.e. more particles are attached to the E-face. E- and P-faces of preexisting membrane at the tips of surface protrusions are particle-free. Nascent membrane fracture faces are more difficult to obtain, but in chilled eggs the membrane splits over much larger areas than in unchilled eggs. Fracture faces of the nascent membrane are sparsely seeded with particles. These items will be sequentially discussed.

The size of the intramembranous particles is unusual, but particles as large as 115–180 Å have been reported earlier for other biological membranes [12–17]. The possibility that proteolytic enzyme or cytochalasin treatment might have given rise to enlarged particles could be excluded by control experiments. Other reports that cytochalasin has no effect on the particle pattern have been published [18, 19]. Moreover, particles of approx. 120 Å in the plasma membrane of ectoderm cells of an amphibian embryo (*Rana pipiens* neurula) have been mentioned before [20].

Intramembranous particles (diameter approx. 80 Å) found in a variety of biological membranes (thickness approx. 75 Å) are thought at least in part to represent proteins and/or glycoproteins complexed with lipids, which float in the lipid bilayer (21–26). Nothing is known about the nature or the function of the 75–180 Å particles seen in the *Xenopus* egg plasma membrane. They probably do not contain proteins that facilitate the permeation of ions, because it is known from previous studies [2] that the preexisting membrane of the *Xenopus* egg is highly impermeable (specific resistance 75 $k\Omega \cdot cm^2$).

The fracture faces of preexisting plasma membrane unambiguously show an unusual distribution of particles, i.e. more particles are attached to the E-face (density

1600–2200 particles/μm^2) than to the P-face (density approx. 300 particles/μm^2). Such a reversed polarity in particle distribution has been reported earlier for the infixed plasma membrane of endothelial cells [27] but not for amphibian embryonic cells [20]. From our material the conclusion that the polarity is reversed appears inevitable, but an interpretation is not yet possible. Further studies will be necessary to elucidate if and when during development the polarity becomes reversed, and if so, whether this is correlated with a change in membrane function, e.g. specific membrane resistance.

Smooth-surfaced areas are thought to represent domains mainly consisting of lipid [28]. The E-face of the preexisting membrane shows such areas at the tips of the surface extensions. Particle-free areas can be brought about artificially by lowering the ambient temperature [16]. Such a change in particle pattern can be explained by assuming that lipid crystallization and consequent demixing affect the normal protein distribution [29]. However, the cooling rate during freezing by our method is about 200 °C per s, which is too fast to cause particle-free areas to appear [30–32]. Our conclusion is that at the tips of the surface extensions the composition of the preexisting membrane is different, the membrane having a higher lipid/protein ratio.

The fracture faces of the nascent membrane were sparsely seeded with particles. The consistent low particle density (300–500 particles/μm^2) suggests that the ratio of lipid to intrinsic proteins is higher than in the preexisting membrane. Cell membranes formed during nerve axon elongation [33] and during regeneration of cilia in *Tetrahymena* [34] were also found to be particle-poor. It suggests that newly-formed cell membrane is relatively simple initially, and that certain components seen as particles are added later.

From previous studies it is known [2] that the nascent membrane in the *Xenopus* egg is highly permeable for ions (specific resistance 1.85 k$\Omega \cdot cm^2$). The current view holds that intrinsic proteins which penetrate the thickness of the lipid bilayer may function as pathways for ions. The particles seen in the nascent membrane may represent complexes of proteins that function as such. One may also consider the possibility that the packing of the lipids in the bilayer is such that the nascent membrane is still an imperfect permeability barrier. This is based on two kinds of observations. First, in ultrathin sections the trilamellar appearance of the nascent membrane remains indistinct [1], while in the same sections the preexisting membrane shows a distinct trilamellar organization. Second, freeze-fracturing of nascent membrane yields an output in membrane fracture faces that is inferior to what might be expected. Chilling markedly improves the output. Both observations can be explained by assuming that the degree of order of nascent membrane lipids is low. Chilling is then thought to improve the order in the lipid bilayer [30] in such a way that the membrane tend to split over larger areas. This interpretation is speculative and requires to be substantiated by experimental evidence.

A cell cycle-dependent difference in particle density of the plasma membrane has been reported for synchronized L-cells and Chinese hamster cells [35]. The particle density is high during mitosis and during the S and G_2 phases, but shows a steep decline followed by a gradual restoration during G_1. The particle pattern of preexisting membrane at early cleavage in *Xenopus* is not different from that in uncleaved eggs (unpublished). Apparently the assembly of nascent membrane is a local event which does not affect the preexisting membrane. It has been suggested [35] that during the early phase of cytokinesis intussusception of membrane components other than

particles may take place. For the *Xenopus* egg we know now that such a process takes place in the region of the furrow, whereas for L-cells or Chinese hamster cells it is still unknown whether insertion is random or local.

The fact that in the *Xenopus* egg the preexisting and nascent cell membrane are continuous but nevertheless maintain their highly different particle densities is noteworthy in itself. The fact that both membrane regions do not merge gives evidence for the existence of considerable structural stability in the egg plasma membrane.

ACKNOWLEDGEMENTS

Grateful acknowledgement is made to Dr. J. Faber for editorial help, to Miss J. Bijvelt for excellent technical assistance, and to Mrs. E.Wolters, Mrs. E. G. Aleven and Mr. L. Boom for the drawings and the photographs.

REFERENCES

1 Bluemink, J. G. and De Laat, S. W. (1973) J. Cell Biol. 59, 89–108
2 De Laat, S. W. and Bluemink, J. G. (1974) J. Cell Biol. 60, 529–540
3 Singal, K. and Sanders, E. J. (1974) J. Ultrastruct. Res. 47, 433–451
4 Bluemink, J. G. (1971) Cytobiologie 3, 176–187
5 Monroy, A. and Baccetti, B. (1975) J. Ultrastruct. Res. 50, 131–142
6 De Laat, S. W., Luchtel, D. and Bluemink, J. G. (1973) Dev. Biol. 31, 163–177
7 Steinberg, M. (1957) Carnegie Inst. Washington Yearb. 56, 347
8 Spiegel, M. (1951) Anat. Rec. 111, 554
9 Sjöstrand, F. S. (1967) in Electron microscopy of cells and tissues, Part I, p. 200, Academic Press, New York
10 Stockem, W. (1970) Mikroscopie 26, 185–189
11 Branton, D., Bullivant, S., Gilula, N. B., Karnovsky, M. J., Moor, H., Mühlethaler, K., Northcote, D. H., Packer, L., Satir, B., Satir, P., Speth, V., Staehelin, L. A., Steere, R. L. and Weinstein, R. (1975) Science 190, 54–56
12 Goodenough, U. W. and Staehelin, L. A. (1971) J. Cell Biol. 48, 594–619
13 Aldridge, H. C. and Gregg, J. H. (1973) Exp. Cell Res. 81, 407–412
14 Gregg, J. H. and Nesom, M. G. (1973) Proc. Natl. Acad. Sci. U.S. 70, 1630–1633
15 Peracchia, C. (1973) J. Cell Biol. 57, 66–76
16 Wunderlich, F. Speth, V., Batz, W. and Kleinig, H. (1973) Biochim. Biophys. Acta 298, 39–49
17 Pollock, E. G. (1975) J. Cell Biol. 67, Part 2, p. 340a
18 Furcht, L. T. and Scott, R. E. (1974) Exp. Cell Res. 88, 311–318
19 Poste, G., Papahadjopoulos, D., Jacobson, K. and Vail, W. J. (1975) Biochim. Biophys. Acta 394, 520–539
20 Decker, R. S. and Friend, D. S. (1974) J. Cell Biol. 62, 32–47
21 Marchesi, V. T., Tillack, T. W., Jackson, R. L., Segrest, J. P. and Scott, R. E. (1972) Proc. Natl. Acad. Sci. U.S. 69, 1445–1449
22 Pinto Da Silva, P. (1972) J. Cell Biol. 53, 777–787
23 Pinto Da Silva, P., Moss, S. and Fudenberg, H. H. (1973) Exp. Cell Res. 81, 127–138
24 Singer, S. J. and Nicolson, G. L. (1972) Science 175, 720–731
25 Bullivant, S. (1973) in Advanced techniques in biological electron microscopy (J. K. Koehler, ed.), pp. 67–112, Springer Verlag, Berlin
26 Tourtellotte, M. E. and Zupnik, J. S. (1973) Science 179, 84–86
27 Dempsey, G. P., Bullivant, S. and Watkins, W. B. (1973) Science 179, 190–192
28 Deamer, D. W., Leonard, R., Tardieu, A. and Branton, D. (1970) Biochim. Biophys. Acta 219, 47–60
29 Grant, C. W. M. (1975) Biophys. J. 15, 949–952
30 Dupont, Y., Gabriel, A., Chabre, M., Gulik-Krzywicki, T. and Schechter, E. (1972) Nature 238, 331–333

31 Ververgaert, P. H. J. Th. (1973) Ph. D. Thesis, State University Utrecht
32 Verkley, A. J. and Ververgaert, P. H. J. Th. (1975) Ann. Rev. Phys. Chem. 26, 101–122
33 Pfenninger, K. H., and Bunge, R. P. (1974) J. Cell Biol. 63, 180–196
34 Satir, B., Sale, W. S. and Satir, P. (1976) Exp. Cell Res. 97, 83–91
35 Scott, R. E., Carter, R. L. and Kidwell, W. R. (1971) Nat. New Biol. 233, 219–220